METHOD FOR PREDICTION OF MAGNETRON CHARACTERISTICS RELATING FREQUENCY AND OPERATING ANODE VOLTAGE TO POWER OUTPUT

H. W. Welch, Jr.
Engineering Research Institute
University of Michigan

This paper is based on work done for the Signal Corps of the United States Army, under Contract No. DA-36-039 sc-5423.

METHOD FOR PREDICTION OF MAGNETRON CHARACTERISTICS RELATING FREQUENCY AND OPERATING ANODE VOLTAGE TO POWER OUTPUT

H. W. Welch, Jr.
University of Michigan

This paper summarizes the results of theoretical and experimental study of space-charge behavior in the oscillating magnetron. This investigation has been directed toward the attainment of a quantitative understanding of frequency characteristics of the oscillating magnetron, namely, frequency pushing and voltage tuning. A report presenting the results in detail has been issued.[1] What follows is, essentially, a summary of the content of this report.

Posthumus,[2] in 1935, described qualitatively the mechanism by which electrons are focussed into a phase position, relative to the r-f potential between the magnetron anode sets, which permits delivery of energy from the electrons to the circuit. Since the first presentation by Hartree and Stoner[3] of the method for self-consistent field calculations of the space-charge distribution in the oscillating magnetron, it has been theoretically possible to

---

1 H. W. Welch, Jr., "Dynamic Frequency Characteristics of the Magnetron Space Charge; Frequency Pushing and Voltage Tuning," Technical Report No. 12, Electron Tube Laboratory, University of Michigan, Ann Arbor, November 1951.

2 K. Posthumus, "Oscillations in a Split-Anode Magnetron, Mechanism of Generation," Wireless Engineer, Vol. 12, pp. 126-132, 1935.

3 This work is reviewed in detail by Walker in Chapter 6 of Microwave Magnetrons, Massachusetts Institute of Technology, Radiation Laboratory Series, Vol. 6, New York, 1948.

describe quantitatively the mechanism of phase focussing of electrons in the magnetron.

The number of calculations required by the self-consistent field method makes prohibitive the application of the method to the quantitative analysis of practically important magnetron characteristics such as frequency pushing. Methods for small-signal analysis, such as that proposed by Buneman[1] cannot be extended to the large-signal problem. The works of several other investigators have been studied and evaluated.[2] The conceptual picture of the space charge in the multianode magnetron under large-signal conditions, which seems to be generally agreed upon, is that shown in Fig. 1. The anode segments which are shown in this picture are assumed attached to an external circuit which is not shown. The distribution of space charge shown in Fig. 1 corresponds to the π-mode which is so named because there exists a phase difference between the potentials on adjacent segments of π-radians. It is found to be possible to represent this distribution of potential, which is stationary in space, by the Fourier sum of a number of travelling waves which proceed in opposite directions around the interaction space. For the π-mode of operation electrons interact primarily with the fundamental wave which is moving in the direction of the electron drift around the cathode. The velocity is such that the maximum of the wave proceeds from one anode segment to the next in one-half cycle. Electrons with this same velocity are said to be in "synchronism" with the wave. The synchronism angular velocity is defined by

$$\omega_n = \frac{2\pi f}{N} \qquad (1)$$

---

[1] Also described by Walker, op. cit.

[2] See Section 1.3 and Bibliography of Technical Report No. 12, Electron Tube Laboratory, University of Michigan.

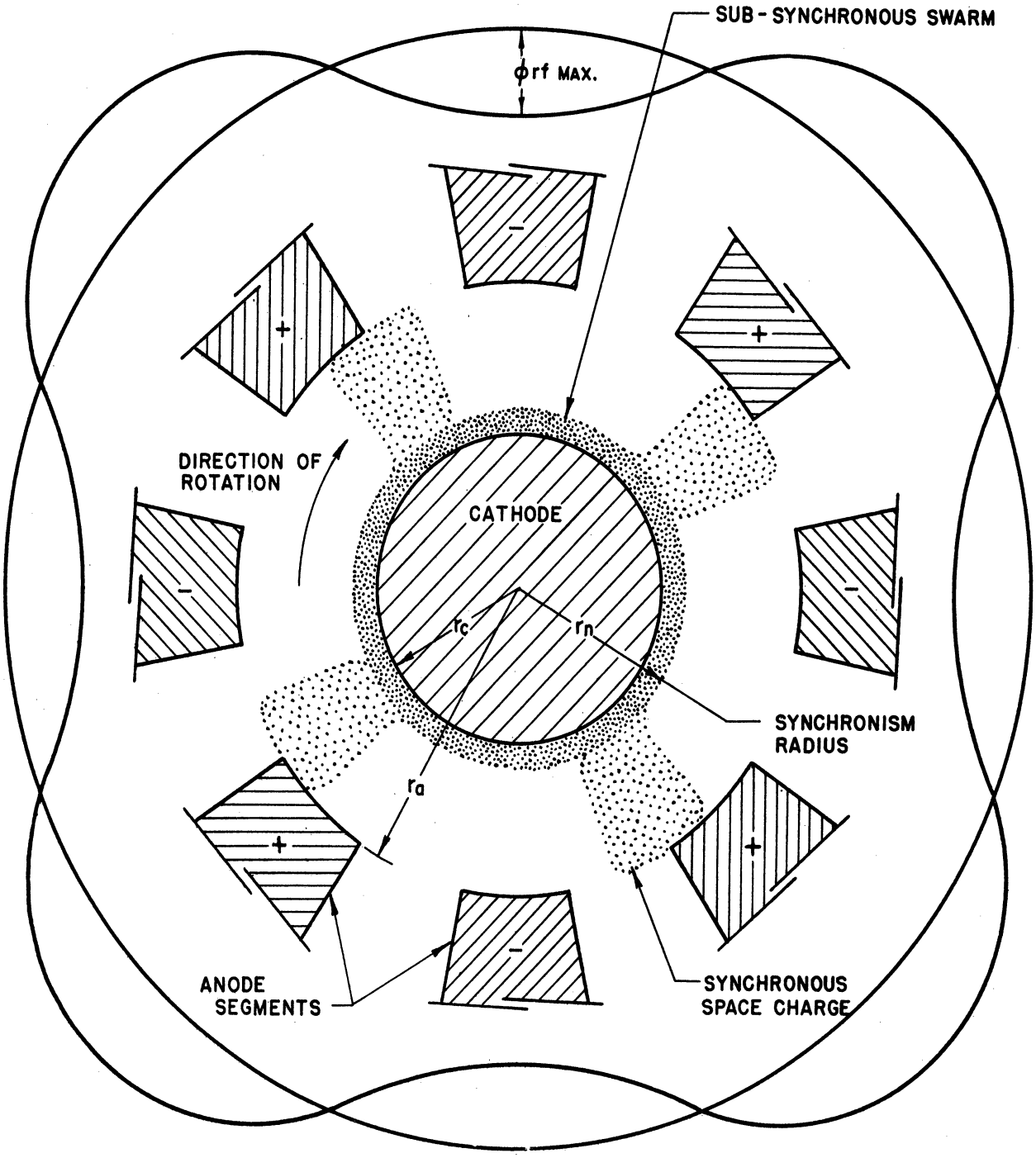

FIG. 1

BASIC PHYSICAL PICTURE OF THE MAGNETRON SPACE CHARGE WITH LARGE SIGNAL R-F POTENTIAL ON THE ANODE

$$n = \frac{N}{2}$$

N = number of anode segments.

The space bounded by the anode segments and the cathode surface is the region of interaction between the electrons and the fields. The presence of the d-c electric and magnetic fields causes the electrons to have a drift motion parallel to the cathode and anode surfaces in this region. The electrons are assumed to leave the cathode surface with zero initial velocities. The synchronism drift velocity must be reached or exceeded at some point in the interaction region if energy is to be delivered to the fundamental travelling-wave component. The conditions for this to be the case have been established for the planar and cylindrical magnetron geometry. In the planar magnetron the synchronism velocity is given by

$$v_n = x_n f \tag{2}$$

where $x_n/2$ is the distance between centers of adjacent anodes.

Since the mathematics of electron behavior is considerably less complicated for the planar magnetron than for the cylindrical magnetron, both have been carried through with the discussion centered around the planar magnetron geometry. The motion of the electron is determined through the force equation which in vector form is

$$\frac{d\vec{v}}{dt} = -\frac{e}{m}\left(\vec{E} + \vec{v} \times \vec{B}\right) \tag{3}$$

$\vec{v}$ = Vector velocity of the electron.

$\vec{E}$ = Vector value of electric field.

$\vec{B}$ = Vector value of magnetic field.

e = Absolute value of electronic charge.

m = Mass of electron.

After a change of variables to the reference frame moving with the synchronism velocity, resolution of the vector values into components, and algebraic manipulation, the force equations in component form become

$$\frac{d}{dt}\left(\frac{1}{2} m v_y^2\right) = e\frac{\partial \phi}{\partial y}\frac{dy}{dt} - Be\,(v_x' + v_n)\,\frac{dy}{dt} \quad , \qquad (4)$$

$$\frac{dv_{x'}}{dt} = \frac{e}{m}\frac{\partial \phi}{\partial x} + \frac{Be}{m}\frac{dy}{dt} \quad , \qquad (5)$$

in the planar system, and

$$\frac{d}{dt}\left(\frac{1}{2} m v_r^2\right) = e\frac{\partial \phi}{\partial r}\frac{dr}{dt} - \left[\, Be(\omega' + \omega_n)\, r - m(\omega' + \omega_n)^2 r\right]\frac{dr}{dt} \quad , \qquad (6)$$

$$\frac{d(\omega' + \omega_n)r}{dt} = \frac{e}{m}\frac{\partial \phi}{\partial \theta} + \left[\frac{Be}{m} - (\omega' + \omega_n)\right]\frac{dr}{dt} \quad , \qquad (7)$$

in the cylindrical system. ϕ is electric potential. The primed values refer to the moving reference frame, i.e.,

$$v_x = v_x' + v_n \qquad (8)$$

$$\omega = \omega' + \omega_n \qquad (9)$$

These equations can be integrated if v_x' and ω' are expressed as functions of distance y, or r. For the static magnetron the result is the cutoff potential. The synchronism anode potential required to bring electrons to the synchronism velocity may also be defined (given by Eq 2.25 and 2.36 in Technical Report No. 12). It is shown that, if a large-signal r-f

potential is present, the electron tends to remain in synchronism after it has reached the synchronism velocity. In this case

$$v_x' = \omega' = 0.$$

By making use of this condition and assuming that the r-f field has negligible effect on the subsynchronous electron it is possible to derive the threshold Hartree potential equation. This potential defines the energy which the electron must receive from the electric field to reach the anode. It is given by

$$\frac{\phi}{\phi_o} = 2\frac{B}{B_o} - 1 \qquad (10)$$

$$\phi_o = \frac{1}{2}\frac{m}{e} v_n^2 \quad \text{for the planar magnetron} \qquad (11)$$

$$\phi_o = \frac{1}{2}\frac{m}{e} \omega_n^2 r_a^2 \quad \text{for the cylindrical magnetron} \qquad (12)$$

$$B_o = \frac{m}{e}\frac{v_n}{y_a} \quad \text{for the planar magnetron} \qquad (13)$$

$$B_o = \frac{2\frac{m}{e}\omega_n}{1 - \frac{r_c^2}{r_a^2}} \quad \text{for the cylindrical magnetron} \qquad (14)$$

y_a = cathode-anode distance

r_c/r_a = ratio of cathode radius to anode radius

The region of the interaction space which is accessible to the electrons is determined by an approximate method. This method makes use of the threshold potential condition and of the fact that electrons may have a component of drift velocity toward the anode when there is an appreciable

component of electric field parallel to the cathode surface. This is the case when there is an r-f potential difference between the anode segments. Electrons are found to drift toward the anode in the region where the r-f electric field is opposing the drift motion parallel to the cathode surface. In the rest of the interaction region, where the r-f electric field is aiding the tangential drift, electrons drift away from the anode. Since all electrons are presumed to originate from the cathode it is assumed that electrons will not exist in the immediate vicinity of the anode in the region where drift motion is away from the anode. Thus two conditions determining the approximate location of the spokes of electrons are established; a certain threshold potential must be exceeded at the anode, and a drift velocity toward the anode must exist at the anode. Application of these principles in a useful graphical construction is illustrated by Fig. 2.

The threshold energy level is represented by the line labeled ϕ_{at}, the actual anode voltage by the line ϕ_a. An r-f potential is represented with peak amplitude ϕ_f. This is the peak value of the fundamental travelling-wave component which appears stationary in the moving reference frame. Fig. 2a illustrates the possibility that, even though the threshold potential is not exceeded by ϕ_a, <u>if</u> an r-f potential exists, the threshold <u>may</u> be exceeded during part of the cycle designated by the interval A-B. In Fig. 2b the effect of the drift velocity condition is illustrated. The drift motion of the electrons is toward the anode in the region C-E and away from the anode in the region D-C. Therefore, although the threshold energy is exceeded in the entire region A-B, electrons can only drift toward the anode in half of this region bounded by C-B. In the region A-C electrons can only exist if they come from the anode, and the

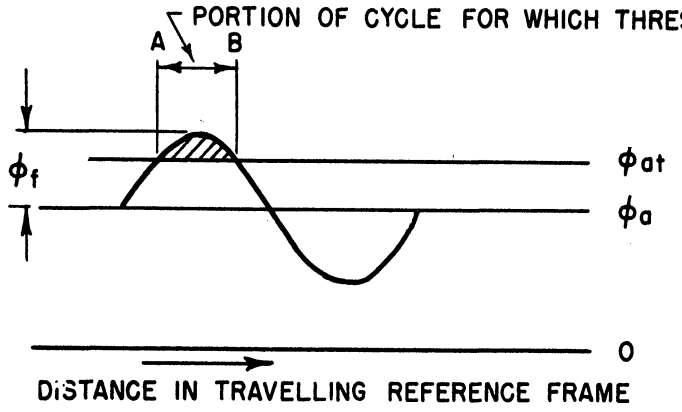

(a)

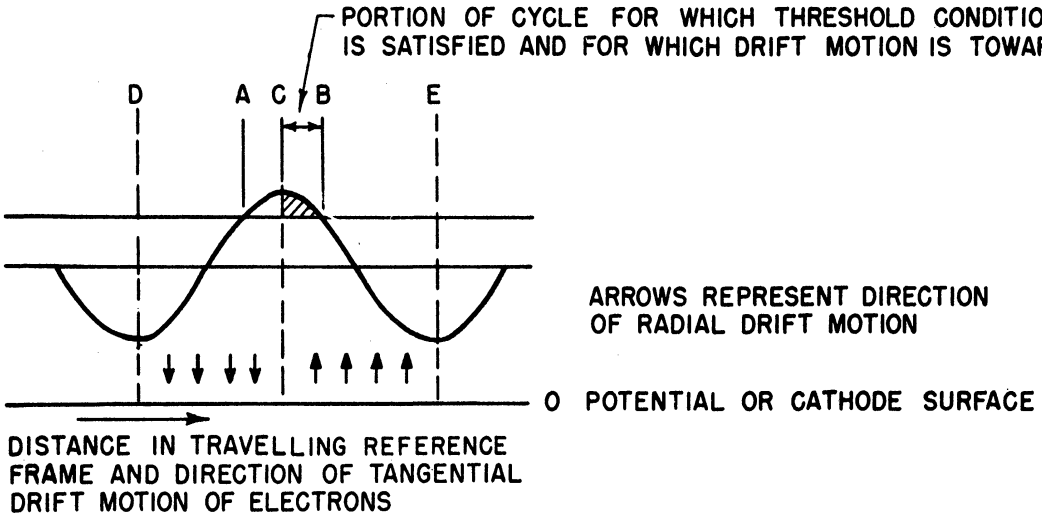

(b)

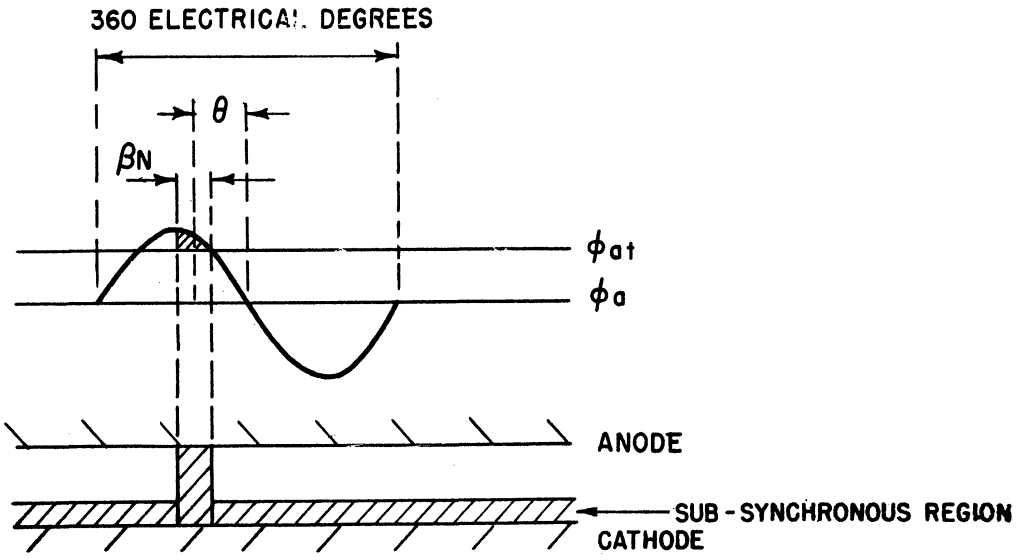

(c)

FIG. 2

ILLUSTRATION OF GRAPHICAL METHOD FOR DETERMINING SPOKE WIDTH AND PHASE ANGLE

assumption is that all electrons are emitted from the cathode. The final picture to be derived from this line of argument is shown in Fig. 2c. Here the potential distribution is plotted over a diagram of the interaction region. The width of the spoke and its phase angle relative to the r-f potential are approximately determined. These quantities are defined by the following symbols which are used when the current induced into the circuit is to be calculated.

θ = phase angle between center of spoke and zero of r-f potential in electrical degrees, negative as shown.

βN = width of spoke in electrical degrees.

β = half the actual space angle width of the spoke.

N = number of anodes.

There are $N/2$ full wavelengths (each 360 electrical degrees) around the cylindrical magnetron structure. The width of a spoke in electrical degrees, therefore is

$$\frac{N}{2} \cdot 2\beta = \beta N$$

The real value in this diagram is in its determination of the angle θ. θ can be shown to be equal to the phase angle between the current induced in the circuit by the motion of the spoke parallel to the anode surface and the r-f potential which is developed between anode sets. In other words, for a particular set of conditions in the "phase focussing" diagram, there is a particular circuit which can produce these conditions since the phase angle and magnitude of the current induced by the spoke will be determined once the anode potential, r-f potential, magnetic field and frequency are determined.

The use of the phase-focussing diagram is illustrated by Figs. 3, 4, 5, and 6. The phase-focussing diagram is in the moving reference frame so that the anode structure which is at rest in the stationary system may be thought of as moving to the left in Fig. 3. The resulting current is shown in Fig. 4. In Fig. 5, the phase-focussing diagrams for a typical volt-ampere characteristic given in 6 are shown. This illustrates space-charge behavior over a typical frequency-pushing characteristic. The significant properties are the large change in frequency and a relatively large change in anode potential. This is exactly the behavior to be expected from operation with a high Q resonant system.

The quantities defined in Fig. 2 may be expressed analytically. Using Fig. 2c we see that

$$- \cos \beta N = \cos 2\theta = \frac{\phi_a - \phi_{at}}{\phi_f} \qquad (15)$$

ϕ_f, the peak value of the fundamental travelling-wave, is related to the actual peak r-f potential between anode segments by a constant which depends only on electrode geometry

$$\phi_f = K \phi_{rf\ max} \qquad (16)$$

A condition of particular interest arises when $\theta = 0$, i.e., when resonance is reached. In this case

$$\phi_a - \phi_{at} = \phi_f \quad ,$$

and the spoke appears as in Fig. 3d or Fig. 5d. For higher d-c potential the potential in the moving reference frame is greater than the threshold value <u>everywhere in the interaction region</u>. It is no longer possible to

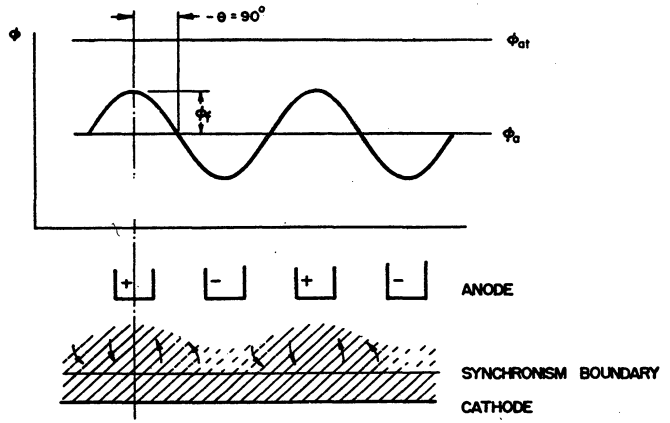

FIG. 3a

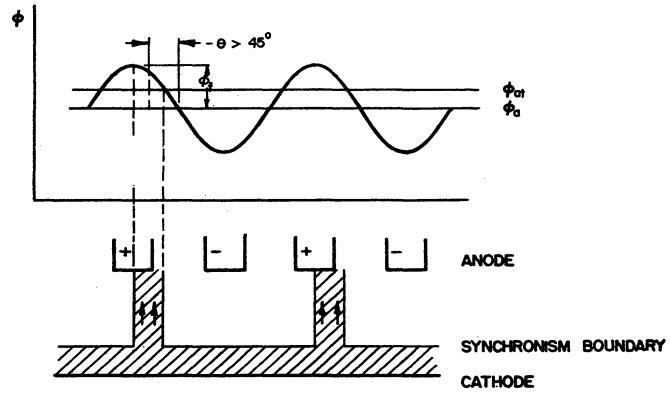

FIG. 3b

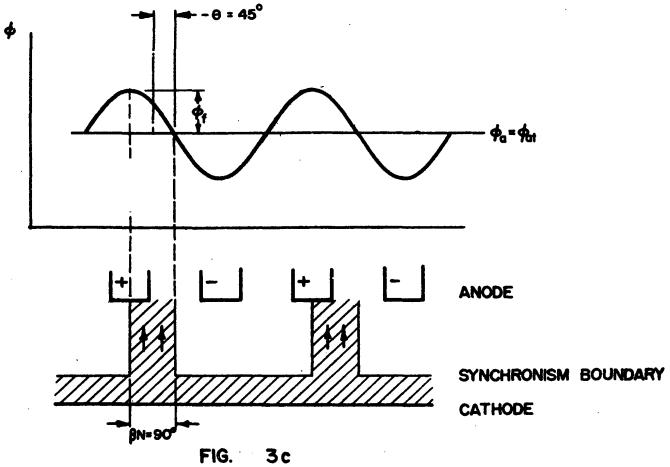

FIG. 3c

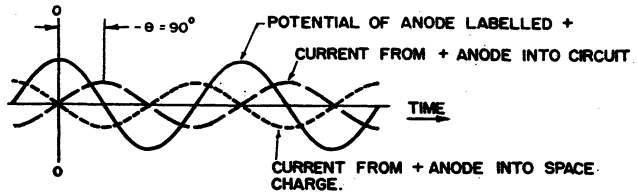

ELECTRONS CAPACITIVE

FIG. 4a

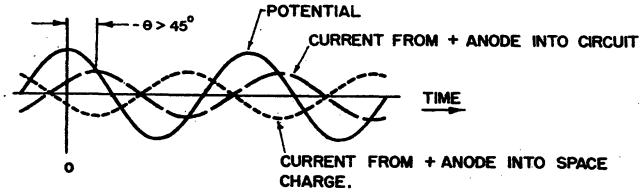

CIRCUIT INDUCTIVE

FIG. 4b

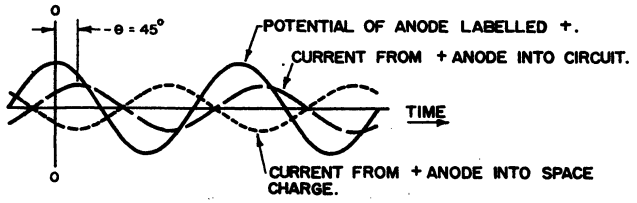

CIRCUIT INDUCTIVE AT HALF POWER POINT.

FIG. 4c

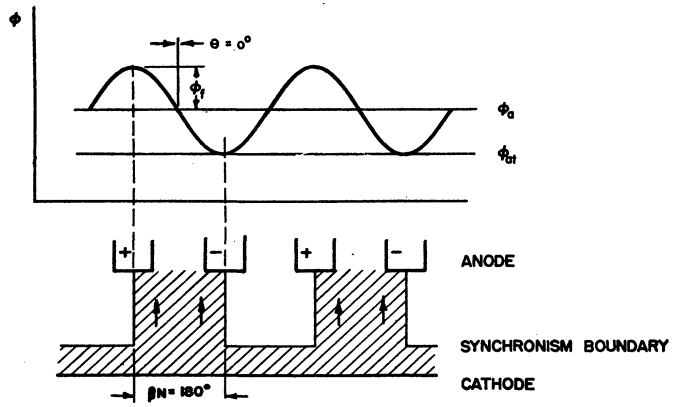

FIG. 3 d

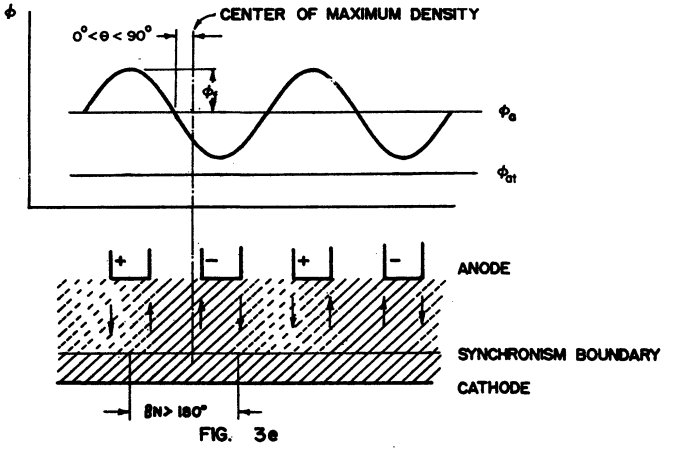

FIG. 3e

FIG. 3

PHASE FOCUSSING DIAGRAM. GRAPHICAL DEVELOPMENT OF RELATIONSHIP BETWEEN PHASE ANGLE θ AND ANODE POTENTIAL. CONSTANT R-F POTENTIAL AND FREQUENCY ARE ASSUMED. ARROWS INDICATE DIRECTION OF ELECTRON DRIFT BETWEEN ANODE AND CATHODE.

THIS FIGURE SHOULD BE STUDIED WITH FIG. 4

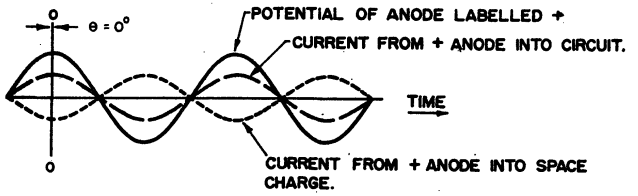

CIRCUIT RESISTIVE ON RESONANCE.

FIG. 4d

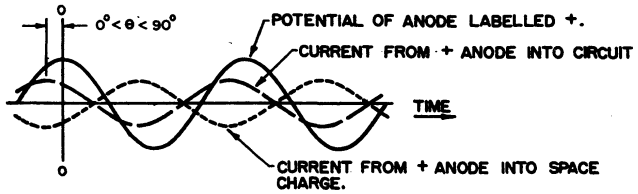

CIRCUIT CAPACITIVE

FIG. 4e

FIG. 4

CURRENT INDUCED BY SPOKE INTO CIRCUIT ON TIME SCALE. TIME 0-0 MARKS THE INSTANT OBSERVED IN ILLUSTRATION LABELLED BY THE SAME LETTER IN FIG. 3.

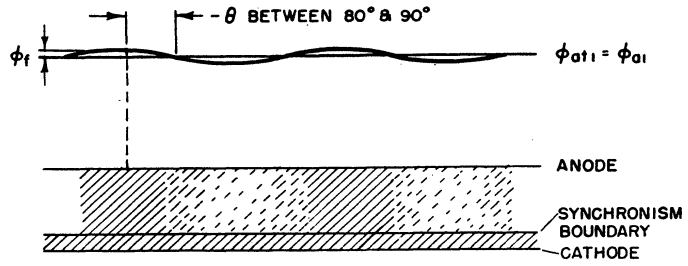

FIG. 5 a

MAGNETRON JUST STARTING. ϕ_f IS VERY SMALL. FREQUENCY IS 5 OR 10 % OFF RESONANCE. BUNCHING NOT COMPLETE, POSSIBLY NOISY OPERATION

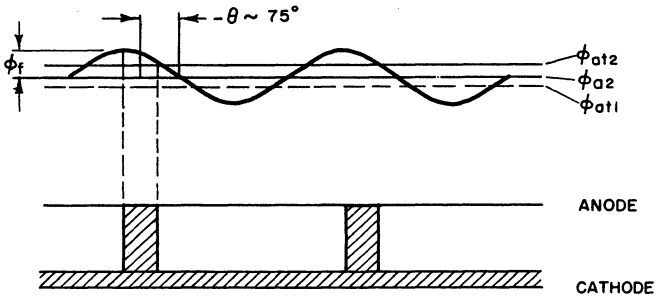

FIG. 5 b

MAGNETRON IS OSCILLATING STRONGLY. ϕ_f IS GREATER THAN 10 % OF ϕ_a. FREQUENCY IS 1 TO 3 % OFF RESONANCE. BUNCHING IS COMPLETE BUT BUNCHES AND INDUCED CURRENT ARE MUCH LESS THAN MAXIMUM.

FIG. 5
PHASE FOCUSSING DIAGRAMS FOR A TYPICAL MAGNETRON VOLT-AMPERE CHARACTERISTIC

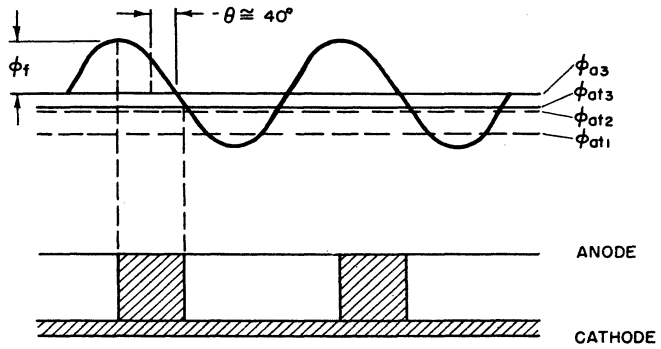

FIG. 5 c

MAGNETRON IS OSCILLATING AT A MEDIUM POWER LEVEL ϕ_f IS 30 OR 40 % OF ϕ_a FREQUENCY IS LESS THAN 1 % OFF RESONANCE. BUNCH HAS INCREASED IN SIZE AND INDUCED CURRENT IS GREATER THAN IN LAST PICTURE

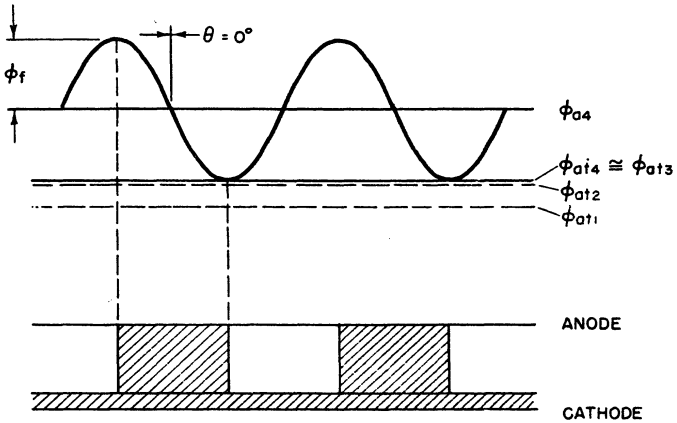

FIG. 5 d

MAGNETRON IS OSCILLATING AT HIGHEST POSSIBLE LEVEL ϕ_f IS OF THE ORDER OF HALF ϕ_a. FREQUENCY IS ON RESONANCE BUNCHES OCCUPY HALF OF THE SPACE. INDUCED CURRENT IS MAXIMUM.

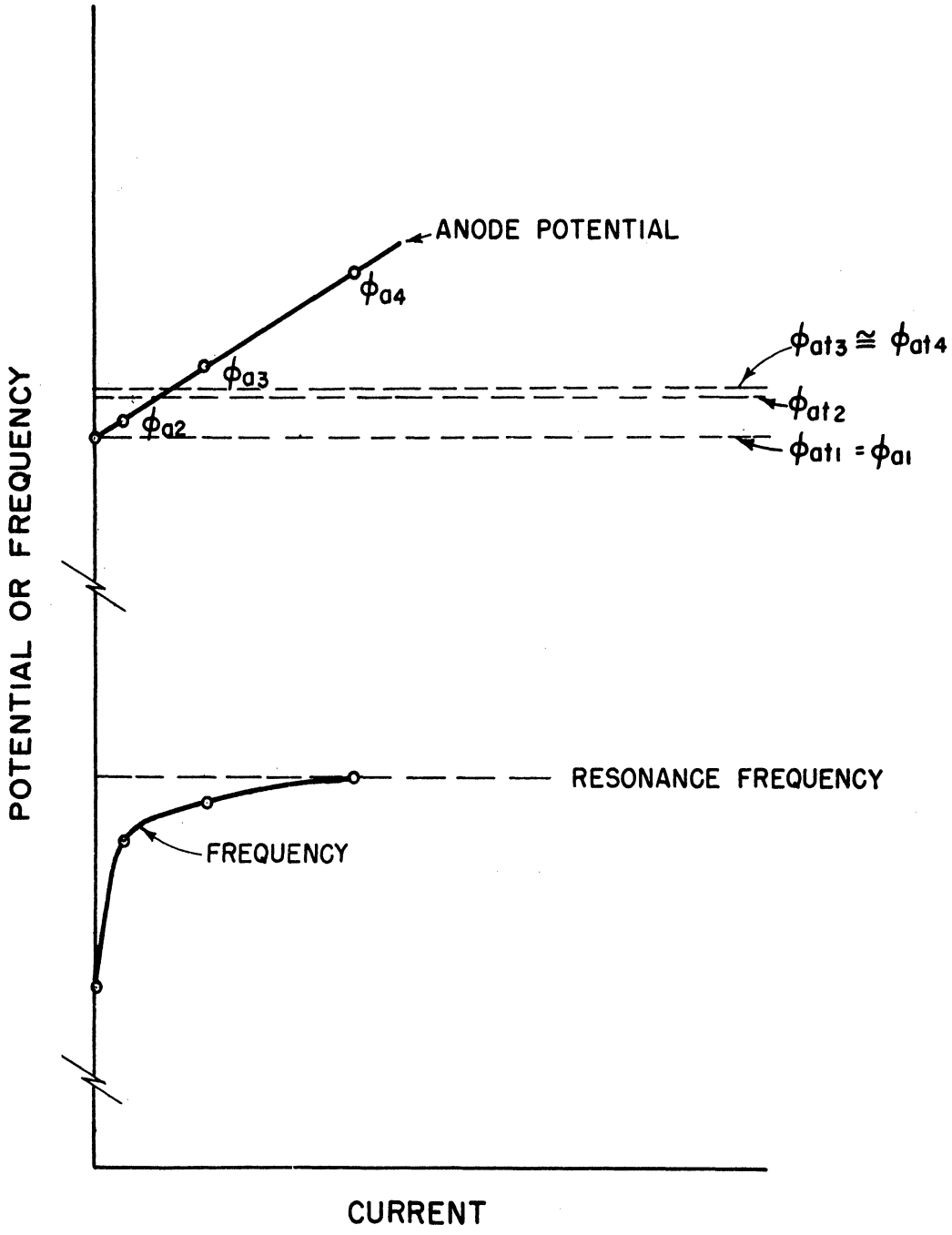

FIG. 6
TYPICAL VOLT-AMPERE CHARACTERISTIC
USED IN MAKING PHASE-FOCUSSING DIAGRAMS
OF FIG. 5

have good phase focussing, and debunching will be expected as illustrated in Fig. 3e. The magnetron will not be expected to oscillate, therefore, when $\phi_a - \phi_{at} > \phi_f$.

Voltage-tuning characteristics correspond to circuits for which the phase angle does not vary rapidly with frequency and to magnetrons with limited d-c current. These conditions have been analyzed and it is found that, as the anode potential is raised, $(\phi_a - \phi_{at})$ remains substantially constant so that the frequency of oscillation is almost directly proportional to the anode potential (through the threshold equation 10). If $\frac{B}{B_o} >> 1$ this proportionality is very near exact.

In order to calculate this current induced in the anode segments it is necessary to estimate the space-charge density in the spokes. Two assumptions are made: the spoke density is assumed to be the average density modified by the ratio of the total volume in the interaction space to the volume occupied by the spokes; the potential distribution determining the average density is assumed to be square-law (this gives a constant charge density). With these assumptions

$$\frac{\beta N}{2\pi} \rho_s = \rho_o \left[1 + \frac{4\varepsilon_o(\phi_a - \phi_{at})}{\rho_o r_c^2 (R_a^2 - R_n^2)} \right] \qquad (17)$$

ρ_s = space-charge density in spokes (coulombs/m3).

$\rho_o = 2\varepsilon_o \frac{m}{e} \omega_n \left(\frac{Be}{m} - \omega_n\right)$.

$R_a = r_a/r_c$.

$R_n = r_n/r_c$ $\quad r_n$ = radius where electrons reach synchronism angular velocity (ω_n).

$$\frac{r_n}{r_c} = \sqrt{\frac{Be/2m}{\frac{Be}{2m} - \omega_n}}$$

Application of the theory of induced currents to the magnetron geometry, using the picture just described, yields finally for magnitude of the current in the external circuit

$$Ig = \frac{K_1}{\frac{\frac{\pi}{2} + \theta}{\cos\theta} - \frac{K_1}{K_2}\frac{\cos 2\theta}{|Y_T|}} \tag{18}$$

$$K_1 = \frac{8}{2}\pi L r_c^2 f \rho_o F(\alpha, N, R_a, R_n) \text{ amperes}$$

$$K_2 = \frac{\rho_o r_c^2 (R_a^2 - R_n^2)}{4\ 2K\varepsilon_o} \text{ volts}$$

$$F(\alpha,N,R_a,R_n) = \frac{\sin\frac{N}{2}\alpha}{\frac{N}{2}\alpha}\frac{1}{R_a^{\frac{N}{2}} - R_a^{\frac{N}{2}}}\left[\frac{R_a^{2+\frac{N}{2}}}{2+\frac{N}{2}} - \frac{R_a^{2-\frac{N}{2}}}{2-\frac{N}{2}} - \frac{R_n^{2+\frac{N}{2}}}{2+\frac{N}{2}} + \frac{R_n^{2-\frac{N}{2}}}{2-\frac{N}{2}}\right],$$

α = angular width of gap between anode segments.

L = length of magnetron cathode.

The potentials have been eliminated from this expression by making use of (15), (16), and

$$\phi_{r\text{-}f} = \frac{I_g}{|Y_T|} \tag{19}$$

$|Y_T|$ = absolute value of circuit admittance as seen between alternate anode sets connected in parallel.

The power in the load is given by

$$P_L = \frac{G_L}{|Y_T|^2}\left(\frac{K_1}{\frac{\frac{\pi}{2} + \theta}{\cos\theta} - \frac{K_1}{K_2}\frac{\cos 2\theta}{|Y_T|}}\right)^2 \tag{20}$$

The d-c anode potential is given by

$$\phi_a - \phi_{at} = \frac{K\sqrt{2}}{|Y_T|} \frac{K_1}{\frac{\frac{\pi}{2} + \theta}{\cos\theta} - \frac{K_1}{K_2}\frac{\cos 2\theta}{|Y_T|}} \cos 2\theta \quad . \qquad (21)$$

These equations have been applied to the particular case of the simple resonant circuit and a non-resonant circuit to calculate frequency-pushing characteristics and voltage-tuning characteristics. A typical set of frequency-pushing characteristics is shown in Figures 7 and 8. The constant A which is referred to is given by

$$A = \frac{K_1}{K_2}\frac{Q_L}{Y_{oc}} \quad . \qquad (22)$$

Y_{oc} = characteristic admittance of a parallel resonant circuit.

A simple parallel resonant circuit is assumed. Figure 7 illustrates the effect of changing Q_L at constant G_L. Figure 8 shows the effect of changing G_L. It is assumed that

$$G_L \simeq \frac{Y_{oc}}{Q_L} \quad .$$

The results agree well with experiment. A number of sets of experimental data have been analyzed and compared with the theory. The effect of cathode temperature on the magnetron behavior has been studied experimentally but very little theoretical explanation is offered.

A general conclusion, resulting from the study, which is a useful rule of thumb in predicting frequency-pushing behavior is the following. The magnetron operating with a high Q resonant system (10 or greater) and under space-charge-limited conditions may be expected to begin appreciable

power generation at approximately 1/10 maximum power at $f_o \times \frac{2}{Q_L}$ megacycles below resonance. f_o is the resonance frequency in megacycles. The range of operation is from this point to between $\frac{f_o}{2Q_L}$ megacycles below resonance and f_o.

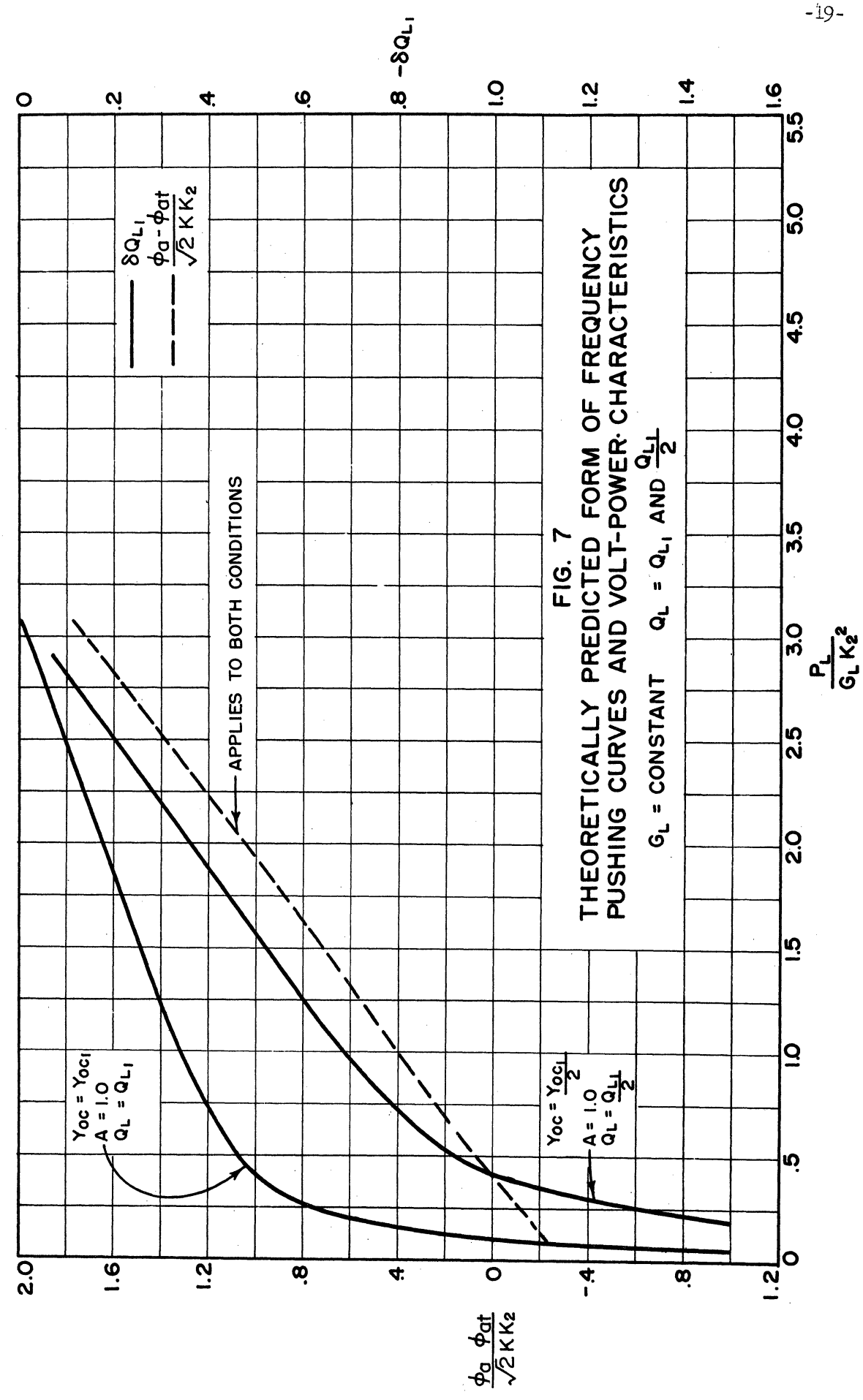
FIG. 7
THEORETICALLY PREDICTED FORM OF FREQUENCY PUSHING CURVES AND VOLT-POWER CHARACTERISTICS
G_L = CONSTANT $Q_L = Q_{L1}$ AND $\frac{Q_{L1}}{2}$
δQ_{L1}
$\frac{\phi_a - \phi_{at}}{\sqrt{2}\,K\,K_2}$
APPLIES TO BOTH CONDITIONS
$Y_{oc} = Y_{oc1}$
$A = 1.0$
$Q_L = Q_{L1}$
$Y_{oc} = \frac{Y_{oc1}}{2}$
$A = 1.0$
$Q_L = \frac{Q_{L1}}{2}$
$\frac{\phi_a\ \phi_{at}}{\sqrt{2}\,K\,K_2}$
$-\delta Q_{L1}$
$\frac{P_L}{G_L K_2^2}$

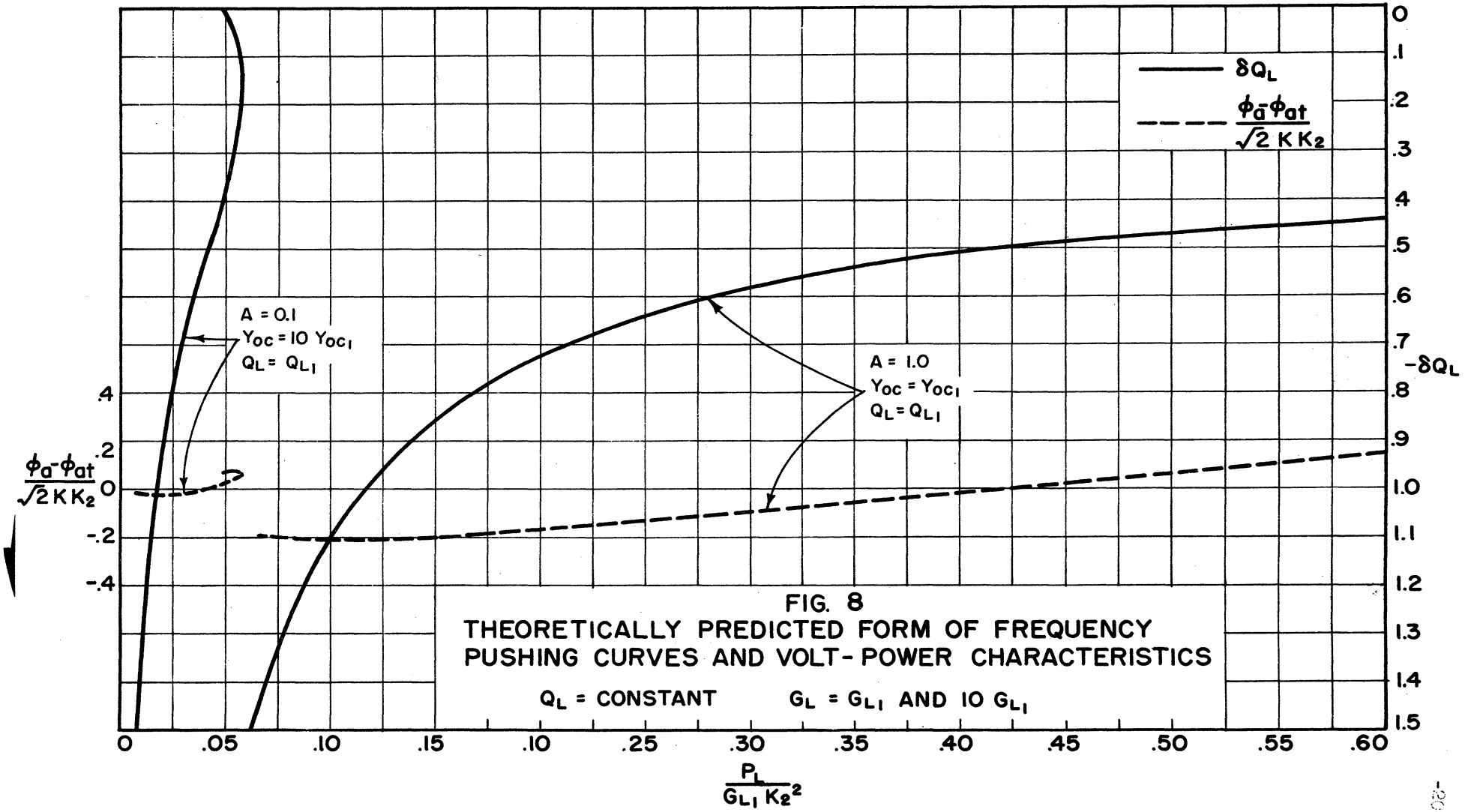

FIG. 8
THEORETICALLY PREDICTED FORM OF FREQUENCY PUSHING CURVES AND VOLT-POWER CHARACTERISTICS

Q_L = CONSTANT $G_L = G_{L1}$ AND $10\ G_{L1}$